Thallium-Gated SPECT in Patients with Major Myocardial Infarction: Effect of Filtering and Zooming in Comparison with Equilibrium Radionuclide Imaging and Left Ventriculography

Pierre Véra, Alain Manrique, Valérie Pontvianne, Anne Hitzel, René Koning and Alain Cribier

Departments of Nuclear Medicine and Cardiology, Charles Nicolle University Hospital, Henri Becquerel Center, Rouen, France

The effect of filtering and zooming on ^{201}Tl-gated SPECT was evaluated in patients with major myocardial infarction. **Methods:** Rest thallium (Tl)-gated SPECT was performed with a 90° dual-head camera, 4 h after injection of 185 MBq ^{201}Tl in 32 patients (mean age 61 ± 11 y) with large myocardial infarction (33% ± 17% defect on bull's eye). End diastolic volume (EDV), end systolic volume (ESV) and left ventricular ejection fraction (LVEF) were calculated using a commercially available semiautomatic validated software. First, images were reconstructed using a 2.5 zoom, a Butterworth filter (order = 5) and six Nyquist cutoff frequencies: 0.13 (B5.13), 0.15 (B5.15), 0.20 (B5.20), 0.25 (B5.25), 0.30 (B5.30) and 0.35 (B5.35). Second, images were reconstructed using a zoom of 1 and a Butterworth filter (order = 5) (cutoff frequency 0.20 [B5.20Z1]) (total = 32 × 7 = 224 reconstructions). LVEF was calculated in all patients using equilibrium radionuclide angiocardiography (ERNA). EDV, ESV and LVEF were measured with contrast left ventriculography (LVG). **Results:** LVEF was 39% ± 2% (mean ± SEM) for ERNA and 40% ± 13% for LVG (*P* = 0.51). Gated SPECT with B5.20Z2.5 simultaneously offered a mean LVEF value (39% ± 2%) similar to ERNA (39% ± 2%) and LVG (40% ± 3%), optimal correlations with both ERNA (*r* = 0.83) and LVG (*r* = 0.70) and minimal differences with both ERNA (−0.9% ± 7.5% [mean ± SD]) and LVG (1.1% ± 10.5%). As a function of filter and zoom choice, correlation coefficients between ERNA or LVG LVEF, and gated SPECT ranged from 0.26 to 0.88; and correlation coefficients between LVG and gated SPECT volumes ranged from 0.87 to 0.94. There was a significant effect of filtering and zooming on EDV, ESV and LVEF (*P* < 0.0001). Low cutoff frequency (B5.13) overestimated LVEF (*P* < 0.0001 versus ERNA and LVG). Gated SPECT with 2.5 zoom and high cutoff frequencies (B5.15, B5.20, B5.25, B5.30 and B5.35) overestimated EDV and ESV (*P* < 0.04) compared with LVG. This volume overestimation with Tl-gated SPECT in patients with large myocardial infarction was correlated to the infarct size. A zoom of 1 underestimated EDV, ESV and LVEF compared with a 2.5 zoom (*P* < 0.02). **Conclusion:** Accurate LVEF measurement is possible with Tl-gated SPECT in patients with major myocardial infarction. However, filtering and zooming greatly influence EDV, ESV and LVEF measurements, and Tl-gated SPECT overestimates left ventricular volumes, particularly when the infarct size increases.

Key Words: gated SPECT; thallium; left ventricular ejection fraction; myocardial infarction

J Nucl Med 1999; 40:513–521

Left ventricular ejection fraction (LVEF) is an important tool in diagnostic and prognostic evaluation of patients with coronary artery disease (*1–3*). Gated SPECT studies offer the potential for simultaneous assessment of myocardial perfusion and function. Gated SPECT has previously been used for LVEF measurement (*4–9*). ^{99m}Tc-sestamibi or ^{99m}Tc-tetrofosmin are widely used in myocardial gated SPECT studies, because they offer the advantages of higher photon energy and higher injectable dose when compared with ^{201}Tl (*10*). However, recent studies have demonstrated the possible use of thallium (Tl)-gated SPECT in patients with suspected or known coronary artery disease, with good correlation between rest LVEF measured with ^{201}Tl and ^{99m}Tc-sestamibi (*11,12*).

LVEF measurement with gated SPECT implies the assessment of left ventricle cavity volume variation. LVEF is then obtained from the end diastolic volume (EDV) and end systolic volume (ESV): LVEF (%) = 100 × (EDV − ESV) / EDV. Thus, accuracy of LVEF measurement is related to the accuracy of EDV and ESV measurements. Determination of left ventricular cavity volume (also referred to as endocardial volume) implies outlining of the corresponding endocardial edge. Semiautomatic (*8,9,13*) and automatic (*12*) methods have been developed to determine endocardial volume. Edge detection methods for volume quantification in SPECT are usually based on thresholding or local gradient operators.

However, SPECT reconstruction parameters may have significant influence on edge detection (*14*). Effects of thresholding have been tested on the gated SPECT measurement of LVEF in humans (*5*), and the effect of filter cutoff frequency has been tested on endocardial volumes in a static

cardiac phantom experiment (4). To our knowledge, the effects of filtering and zooming on gated SPECT LVEF and volume measurements have never been studied in humans, particularly in patients with large myocardial infarction. The aim of this study was to test different cutoff frequencies and reconstruction zooms (previously used in clinical studies) in patients with major myocardial infarction. Gated SPECT LVEF is compared with equilibrium radionuclide angiocardiography (ERNA), and volumes were compared with left contrast ventriculography (LVG).

MATERIALS AND METHODS

Patients

Rest Tl-gated SPECT was performed in 32 consecutive patients (26 men, 6 women, mean age 61 ± 11 y) with documented myocardial infarction 1 wk to 6 mo before the study. All patients were referred to the Nuclear Medicine Department for assessment of myocardial viability. Myocardial infarction was documented by the presence of electrocardiographic Q-waves or cardiac enzyme elevation.

Gated SPECT Acquisition

Myocardial gated SPECT was performed at rest, 4 h after intravenous injection of 185 MBq (5 mCi) ^{201}Tl. SPECT acquisitions were obtained with a dual-head, large-field-of-view gamma camera (DST-XL; SMVi, Buc, France) equipped with low-energy, high-resolution, parallel-hole collimators. Effective resolution with full width at half maximum at 10 cm was 8 mm in air and 9.6 mm in water. The two heads were placed in an L-shaped configuration. Thirty-two projections (16 per head) were obtained as 64 × 64 matrices, using a step-and-shoot acquisition over a 180° arc extending from the 45° right anterior oblique to the 45° left posterior oblique position. Acquisition zoom was 1.33, giving a pixel size of 6.8 × 6.8 mm. The energy windows were 70% ± 20% and 167% ± 20% keV. Images were acquired for 120 s per projection for a total imaging time of 32 min. Images were gated at eight frames per cardiac cycle using an R-wave trigger, and the acceptance window was 100%.

Gated SPECT Data Processing

First, total count density was calculated in a 64 × 64 pixel region of interest (ROI) throughout the total gated SPECT projections. Myocardial count density was calculated in a 16 × 64 pixel ROI located in the myocardial area throughout the total gated SPECT projections. Second, a commercially available semiautomated gated SPECT processing software was used to reconstruct gated SPECT (Vision software revision 4.1.0, Multidim®; SMVi). Images were reconstructed from projection data using the filtered backprojection algorithm with a centered software zoom of 2.5 (Z2.5; 2.7 × 2.7 mm pixel size) and a Butterworth filter with an order of 5. Six cutoff frequencies of 0.13, 0.15, 0.20, 0.25, 0.30 and 0.35 cycle/pixel were successively tested (B5.13, B5.15, B5.20, B5.25, B5.30 and B5.35). This range of cutoff frequencies was chosen because cutoff frequencies <0.13 or >0.35 cycle/pixel provide aberrant images with the software used and because these values have been previously used in clinical studies (see Discussion section). A software zoom of 1 (6.8 × 6.8 mm pixel size) was used with the Butterworth filter with an order of 5 and cutoff frequency of 0.20 cycle/pixel (B5.20Z1). Zoom 2.5 and 1 were successively tested on the basis of the two commercially available

software specifications proposed by the manufacturer on our workstation: Multidim® (Z2.5) and QGS® (Z1) (Vision software revision 4.1.0; SMVi). A total of 224 reconstructions were performed (7 reconstructions for each of 32 patients). Background subtraction and attenuation correction were not used. With this software (Multidim®), the endocardial edge was defined as the maxima of the first derivatives of the squared activity profiles, searching from the center of the myocardial cavity. The endocardial edge distance D was defined as $D_{endo} = maxima[dA^2(l)/dl]$, with A(l) as the activity profile for a given vector (ll) and d as derivative. This commercially available software was previously described (15) and validated (11). The volumes were calculated from the endocardial surfaces for each time segment. EDV, ESV and LVEF were calculated for the six cutoff frequencies and for the two zooms. The intra- and interobserver variabilities of the technique were examined in all patients for LVEF, EDV and ESV.

Quantification of Infarct Size

All gated tomograms were added at each projection angle to produce a summed tomographic dataset similar to that which would have been acquired without gating. Summed tomograms were reconstructed using a filtered backprojection algorithm, B5.20 filter and 2.5 zoom. The infarct size was quantified on a bull's eye polar map with a fully automatic procedure, as described previously (16). Briefly, a 60% level isocontour of the maximal value was generated on the bull's eye. This isocontour divided the bull's eye polar map into two ROIs: the area of normal Tl uptake (pixels with values >60% of the maximum) and Tl defect (pixels with values <60% of the maximum). The infarct size was expressed as the percentage of pixel values <60% on the total bull's eye area.

Equilibrium Radionuclide Angiocardiography

All patients underwent planar ERNA immediately after Tl-gated SPECT. ERNA acquisition was obtained with a single-head gamma camera (DS7; SMVi) equipped with a low-energy, all-purpose, parallel-hole collimator. Human serum albumin, labeled with 925 MBq (25 mCi) ^{99m}Tc in a volume of 1 mL, was administered through an indwelling catheter placed in the antecubital vein. Patients were positioned in the supine position with the camera in a 30°–45° left oblique projection, with a 5°–10° caudal tilt, to maximize the separation of ventricular images. Images were gated at 16 frames per cardiac cycle using an R-wave trigger. A total of 350,000 counts were obtained for each frame with a zoom factor of 2 in a 64 × 64 acquisition matrix. LVEF was calculated using standard, automatic, commercially available software (Sophy NXT, Software revision 2.01; SMVi). LVEFs were defined automatically for 30 patients. For 2 patients, ventricular ROIs were corrected manually. Accuracy and reproducibility of this software were previously validated in our center on 15 healthy subjects and 58 patients with heart failure. With this software and in the previous study, normal LVEF values were 77% ± 5% (mean ± SD), and intra- and interobserver correlation coefficients were r = 0.98 and r = 0.97, respectively (17).

Left Ventriculography

Single-plane digital angiograms were obtained in the 30° right anterior oblique position using the Philips digital cardiac imaging system (Philips Medical Systems International BV, Da Best, The Netherlands), at 30 frames/s. Endocardial borders were automatically determined at end diastole and end systole, and manually corrected when necessary. EDV, ESV and LVEF were calculated using the Sandler and Dodge method (18). In 7 patients, cardiac

events occurred between LVG and gated SPECT. These 7 LVGs were then excluded from the study.

Statistics

Means (M) and SD or SEM were used for descriptive statistics. Paired EDV, ESV and LVEF were analyzed by analysis of variance with repeated measures. The paired-post hoc t test was performed for multiple tests when necessary. Correlation (r) and linear regression between ERNA, LVG and Tl-gated SPECT were calculated. Agreement between ERNA, LVG and Tl-gated SPECT was assessed using Bland-Altman analysis (19). Data were expressed as mean value ± 1 SD (M ± SD%). Linear regressions of the Bland-Altman plots were calculated. All linear regressions were expressed as y = a.x + b, with a as the slope and b the intercept of the line. SD of the slopes and intercepts were calculated. $P \leq 0.05$ was considered significant.

RESULTS

Reconstructions were performed semiautomatically in all patients. Count density in Tl-gated SPECT was $11 \times 10^6 \pm 3 \times 10^6$ (M ± SD) counts in the total acquisition and $2.8 \times 10^6 \pm 0.7 \times 10^6$ counts in the myocardial area.

Infarct size was 33% ± 17% of the myocardial surface (M ± SD). The infarction location was anterior in 14 patients, posterior in 15 and lateral in 3. Mean LVEF was 39% ± 2% for ERNA (M ± SEM) and 40% ± 3% for LVG ($P = 0.51$).

Intra- and Interobserver Reproducibilities

Intra- and interobserver differences in gated SPECT (B5.20Z2.5) were minor for LVEF, EDV and ESV, with excellent correlation coefficients (respectively 0.96, 0.99 and 0.99 for intraobserver reproducibility, and 0.88, 0.98 and 0.99 for interobserver reproducibility). Intercepts were close to a value of 0, and regression line slopes were close to a value of 1 (Appendix Table 1).

Relations Between Equilibrium Radionuclide Angiocardiography, Left Ventriculography and Tl-Gated SPECT

Linear regression analysis between ERNA, LVG and Tl-gated SPECT are shown in Table 1. Correlation coefficients between ERNA LVEF and Tl-gated SPECT LVEF ranged from 0.75 to 0.88. Correlation coefficients between LVG LVEF and Tl-gated SPECT LVEF ranged from 0.26 to 0.72. Correlation coefficients between LVG volumes and Tl-SPECT volumes ranged from 0.87 to 0.94.

Blant-Altman analyses between ERNA, LVG and Tl-gated SPECT are shown in Table 2. Mean differences (±SD) between ERNA LVEF and Tl-gated SPECT LVEF ranged from −13.6% ± 13.1% to 5.4% ± 7.4%. Mean difference (±SD) between LVG LVEF and Tl-gated SPECT LVEF ranged from −12.6% ± 16.0% to 6.7% ± 15.0%. For LVEF, linear regression analyses of Blant-Altman plots showed no systematic correlation between LVG gated SPECT difference and mean LVG gated SPECT (except for B5.13 and B5.15). Mean differences (±SD) between LVG volumes and Tl-gated SPECT volumes ranged from −94 ± 87 mL to 0 ± 61 mL. For volumes, linear regression analysis of Blant-Altman plots showed a significant relationship between

LVG gated SPECT difference and mean LVG gated SPECT. This relationship demonstrated that the overestimation of volumes with Tl-gated SPECT was related to the volume size. (An example of Bland-Altman plots for EDV and ESV are given in Appendix Fig. 1.)

Gated SPECT with B5.20Z2.5 simultaneously offers a mean LVEF value (39% ± 2%) similar to ERNA (39% ± 2%) and LVG (40% ± 3%), optimal correlations with both ERNA ($r = 0.83$) and LVG ($r = 0.70$) (Table 1) and minimal differences with both ERNA (M ± SD = −0.9% ± 7.5%) and LVG (M ± SD = 1.1% ± 10.5%) (Table 2).

Effect of Filtering and Zooming of Left Ventricular Ejection Fraction

Filtering and zooming have a significant effect on LVEF measurement (Fig. 1). Using low cutoff frequencies overestimated LVEF compared with ERNA, LVG and gated SPECT reconstructed with high cutoff frequencies. B5.13 LVEF was significantly higher than LVG LVEF ($P < 0.0001$), ERNA LVEF ($P < 0.0001$) and all other gated SPECT reconstructions ($P < 0.0001$). B5.15 LVEF was significantly higher than B5.25 LVEF ($P = 0.013$), B5.30 LVEF ($P = 0.009$) and B5.35 LVEF ($P = 0.006$). A reconstruction zoom of 1 (B5.20Z1) underestimated LVEF compared with gated SPECT studies with software zoom of 2.5 for the same reconstruction filter ($P = 0.008$).

Effect of Filtering and Zooming on End Diastolic Volume

Filtering and zooming have a significant effect on EDV (Fig. 2A). Tl-gated SPECT overestimated EDV compared with LVG. LVG EDV was significantly lower than B5.13 ($P < 0.0001$), B5.15 ($P = 0.033$), B5.20 ($P < 0.0001$), B5.25 ($P < 0.0001$), B5.30 ($P < 0.0001$) and B5.35 EDV ($P < 0.0001$). B5.35 EDV was significantly higher than B5.25 ($P = 0.006$), B5.20 ($P = 0.0001$), B5.15 ($P < 0.0001$) and B5.13 EDV ($P = 0.001$). B5.30 EDV was also significantly higher than B5.20 ($P = 0.002$), B5.15 ($P < 0.0001$) and B5.13 EDV ($P = 0.0008$). B5.25 EDV was significantly higher than B5.15 EDV ($P = 0.003$). Software zoom of 1 (B5.20Z1) underestimated EDV compared with 2.5 zoom software for the same reconstruction filter ($P = 0.0002$).

Effect of Filtering and Zooming on End Systolic Volume

Filtering and zooming have a significant effect on ESV (Fig. 2B). Tl-gated SPECT tended to overestimate ESV compared with LVG. LVG ESV was significantly lower than B5.15 ($P = 0.04$), B5.20 ($P = 0.002$), B5.25 ($P < 0.0001$), B5.30 ($P < 0.0001$) and B5.35 EDV ($P < 0.0001$). B5.35 ESV was significantly higher than B5.20 ($P = 0.0002$), B5.15 ($P < 0.0001$) and B5.13 ESV ($P < 0.0001$). B5.30 ESV was also significantly higher than B5.20 ($P = 0.002$), B5.15 ($P < 0.0001$) and B5.13 ESV ($P < 0.0001$). B5.25 ESV was significantly higher than B5.20 EDV ($P = 0.03$), B5.15 EDV ($P < 0.0001$) and B5.13 ESV ($P = 0.0002$). B5.20 ESV was significantly higher than B5.13 ESV ($P = 0.01$). Software zoom of 1 (B5.20Z1) underestimated ESV

TABLE 1
Results of Linear Regression Analysis Between ERNA, LVG and Thallium-Gated SPECT

		Thallium-gated SPECT						
		Z1	**Z2.5**					
ERNA	**LVEF**	**B5.20**	**B5.13**	**B5.15**	**B5.20**	**B5.25**	**B5.30**	**B5.35**
	a ± SE	0.85 ± 0.14	0.44 ± 0.05	0.63 ± 0.06	0.70 ± 0.09	0.61 ± 0.09	0.71 ± 0.09	0.67 ± 0.09
	b ± SE	10.5 ± 4.9	15.7 ± 2.8	11.5 ± 3.0	11.0 ± 3.8	15.9 ± 3.9	11.7 ± 3.9	14.0 ± 3.8
	r	0.75	0.86	0.88	0.83	0.76	0.81	0.80
	F	35.48	78.16	94.25	58.69	39.68	53.86	48.39
	P	<0.0001	<0.0001	<0.0001	<0.0001	<0.0001	<0.0001	<0.0001
LVG	**LVEF**	**B5.20**	**B5.13**	**B5.15**	**B5.20**	**B5.25**	**B5.30**	**B5.35**
	a ± SE	0.38 ± 0.29	0.45 ± 0.09	0.58 ± 0.15	0.82 ± 0.17	0.60 ± 0.18	0.70 ± 0.18	0.62 ± 0.18
	b ± SE	26.9 ± 10.2	16.2 ± 5.1	15.0 ± 6.8	7.8 ± 7.2	17.3 ± 7.1	13.9 ± 7.0	16.8 ± 7.2
	r	0.26	0.72	0.62	0.70	0.57	0.63	0.57
	F	1.73	25.32	14.82	21.53	11.10	14.86	11.33
	P	0.20	<0.0001	0.0008	<0.0001	0.0029	0.0008	0.0027
LVG	**EDV**	**B5.20**	**B5.13**	**B5.15**	**B5.20**	**B5.25**	**B5.30**	**B5.35**
	a ± SE	0.57 ± 0.06	0.43 ± 0.05	0.50 ± 0.04	0.50 ± 0.05	0.52 ± 0.06	0.54 ± 0.06	0.45 ± 0.05
	b ± SE	81 ± 15	89 ± 14	83 ± 11	73 ± 14	58 ± 16	41 ± 17	62 ± 17
	r	0.87	0.88	0.93	0.90	0.87	0.89	0.87
	F	74.56	80.53	148.20	89.08	78.14	87.55	75.78
	P	<0.0001	<0.0001	<0.0001	<0.0001	<0.0001	<0.0001	<0.0001
LVG	**ESV**	**B5.20**	**B5.13**	**B5.15**	**B5.20**	**B5.25**	**B5.30**	**B5.35**
	a ± SE	0.62 ± 0.06	0.47 ± 0.03	0.52 ± 0.04	0.52 ± 0.04	0.53 ± 0.04	0.55 ± 0.05	0.51 ± 0.05
	b ± SE	37 ± 10	57 ± 7	49 ± 7	38 ± 7	28 ± 9	21 ± 10	25 ± 11
	r	0.90	0.94	0.94	0.94	0.93	0.92	0.90
	F	105.42	165.04	171.22	204.15	141.75	122.50	108.28
	P	<0.0001	<0.0001	<0.0001	<0.0001	<0.0001	<0.0001	<0.0001

ERNA = equilibrium radionuclide angiography.
LVEF = left ventricular ejection fraction.
LVG = left contrast ventriculography.
EDV = end diastolic volume.
ESV = end systolic volume.
F = F value.
a ± SE = slope of linear regression ± SE.
b ± SE = intercept of linear regression ± SE.

compared with 2.5 zoom software for the same reconstruction filter ($P = 0.02$).

DISCUSSION

This study demonstrates that accurate LVEF measurement may be obtained with Tl-gated SPECT in patients with major myocardial infarction. However, filtering and zooming greatly influence EDV, ESV and LVEF measurements, and Tl-gated SPECT overestimates EDV and ESV in patients with major myocardial infarction.

Because LVEF is a fundamental parameter for diagnosis and prognosis in patients with coronary artery disease, accurate determination of LVEF is important, especially in patients with severe myocardial scar. Therefore, gated SPECT was tested in patients with major myocardial infarction and/or left ventricular dysfunction.

This study was performed with [201]Tl. Although techne-

tium agents are widely used in myocardial gated-SPECT studies, ^{201}Tl remains the main radionuclide for myocardial studies in the U.S. ([12]). Two principal reasons explain this phenomenon: (a) increased Tl lung uptake with stress is associated with decreased left ventricular function, multivessel or severe coronary disease and poor prognosis ([20–24]), and (b) ^{201}Tl is widely considered to be the agent of choice for identifying myocardial viability ([25,26]). Nevertheless, ^{201}Tl was preferred in our patients referred for evaluation of myocardial viability. A gated SPECT study was performed to assess simultaneously rest perfusion and function in these patients.

Technetium agents are also widely used in myocardial gated-SPECT studies, because they offer the advantages of higher injectable dose compared with ^{201}Tl, as well as a higher myocardial count density. A recent study showed accurate and comparable LVEF and volume measurements

TABLE 2
Results of Bland-Altman Analysis Between ERNA, LVG and Thallium-Gated SPECT

ERNA	LVEF	Thallium-gated SPECT						
		Z1	Z2.5					
		B5.20	B5.13	B5.15	B5.20	B5.25	B5.30	B5.35
	M ± SD	5.4 ± 7.4	−13.6 ± 13.1	−4.2 ± 7.6	−0.9 ± 7.5	1.1 ± 8.9	1.0 ± 7.3	1.9 ± 7.9
	a ± SE	0.14 ± 0.14	−0.68 ± 0.09	−0.34 ± 0.09	−0.19 ± 0.12	−0.26 ± 0.14	−0.13 ± 0.12	−0.19 ± 0.13
	b ± SE	0.2 ± 5.4	17.7 ± 4.5	9.7 ± 4.0	6.5 ± 4.9	10.9 ± 5.5	6.1 ± 4.9	8.9 ± 5.0
	r	0.19	−0.81	−0.56	−0.28	−0.34	−0.20	−0.27
	F	1.00	53.29	12.90	2.46	3.55	1.21	2.15
	P	0.32	<0.0001	0.0012	0.12	0.07	0.20	0.15
LVG	LVEF	B5.20	B5.13	B5.15	B5.20	B5.25	B5.30	B5.35
	M ± SD	6.7 ± 15.0	−12.6 ± 16.0	−2.5 ± 12.8	1.1 ± 10.5	2.6 ± 12.9	2.8 ± 11.8	2.8 ± 12.7
	a ± SE	0.59 ± 0.30	−0.54 ± 0.16	−0.08 ± 0.20	0.20 ± 0.18	0.08 ± 0.22	0.14 ± 0.20	0.10 ± 0.22
	b ± SE	−14.8 ± 11.3	12.1 ± 7.7	0.8 ± 8.6	−6.8 ± 7.2	−0.3 ± 8.8	−2.4 ± 8.0	−1.0 ± 8.7
	r	0.38	−0.58	−0.08	0.24	0.07	0.14	0.09
	F	3.86	11.71	0.16	1.31	0.11	0.47	0.20
	P	0.06	0.0023	0.69	0.26	0.73	0.50	0.65
LVG	EDV	B5.20	B5.13	B5.15	B5.20	B5.25	B5.30	B5.35
	M ± SD	0 ± 61	−47 ± 95	−23 ± 74	−43 ± 74	−64 ± 70	−84 ± 65	−94 ± 87
	a ± SE	−0.44 ± 0.10	−0.73 ± 0.09	−0.61 ± 0.07	−0.58 ± 0.09	−0.54 ± 0.10	−0.50 ± 0.09	−0.67 ± 0.10
	b ± SE	84 ± 22	110 ± 22	102 ± 17	82 ± 22	56 ± 20	34 ± 24	66 ± 25
	r	−0.66	−0.86	−0.87	−0.80	−0.75	−0.74	−0.82
	F	18.02	63.15	72.22	40.32	29.40	28.34	48.41
	P	<0.0001	<0.0001	<0.0001	<0.0001	<0.0001	<0.0001	<0.0001
LVG	ESV	B5.20	B5.13	B5.15	B5.20	B5.25	B5.30	B5.35
	M ± SD	−14 ± 50	−12 ± 77	−18 ± 66	−34 ± 64	−52 ± 63	−61 ± 60	−67 ± 68
	a ± SE	−0.39 ± 0.09	−0.67 ± 0.07	−0.59 ± 0.07	−0.59 ± 0.06	−0.55 ± 0.07	−0.52 ± 0.08	−0.58 ± 0.08
	b ± SE	32 ± 14	73 ± 11	59 ± 11	45 ± 11	29 ± 13	18 ± 14	23 ± 15
	r	−0.68	−0.90	−0.88	−0.89	−0.84	−0.80	−0.82
	F	19.51	100.40	76.51	87.88	54.41	42.00	48.11
	P	<0.0001	<0.0001	<0.0001	<0.0001	<0.0001	<0.0001	<0.0001

ERNA = equilibrium radionuclide angiography.
LVEF = left ventricular ejection fraction.
LVG = left contrast ventriculography.
EDV = end diastolic volume.
ESV = end systolic volume.
F = F value.
M ± SD = mean of difference between reference, method (ERNA or LVG) and thallium-gated SPECT.
a ± SE = slope of linear regression of Bland-Altman plot ± SE.
b ± SE = intercept of the linear regression of Bland-Altman plot ± SE.

with ^{201}Tl compared with ^{99m}Tc, when count density was greater than 500,000 counts in the myocardial area (27). To obtain higher image quality and higher count density in our gated SPECT, each projection was obtained during 120 s. During 120 s and with 185 MBq (5 mCi) injected, a total 2.8 × 10⁶ ± 0.7 × 10⁶ counts (M ± SD) were obtained in the myocardial area. However, because most laboratories use less injected activity (except for re-injection protocols), the optimal filters found in this study are possibly not adapted for higher noise-to-signal ratio images associated with lower injected activity, even with the same camera and collimators.

This study also demonstrates that Tl-gated SPECT is feasible in patients with major myocardial infarction. Recon-structions were performed semiautomatically in all patients. Gated SPECT with B5.20Z2.5 simultaneously offers mean LVEF value (39% ± 2%) similar to ERNA (39% ± 2%) and LVG (40% ± 3%), optimal correlations with both ERNA ($r = 0.83$) and LVG ($r = 0.70$) (Table 1), and minimal mean differences with both ERNA (M ± SD = −0.9% ± 7.5%) and LVG (M ± SD = 1.1% ± 10.5%) (Table 2). Correlations between Tl-gated SPECT LVEF and ERNA LVEF were considered acceptable (range 0.75–0.88). Correlations were less satisfactory with LVG LVEF.

Several studies have been reported with gated SPECT. Tracers, injected doses, acquisition protocols and reconstruction parameters were generally different (Appendix Table 2).
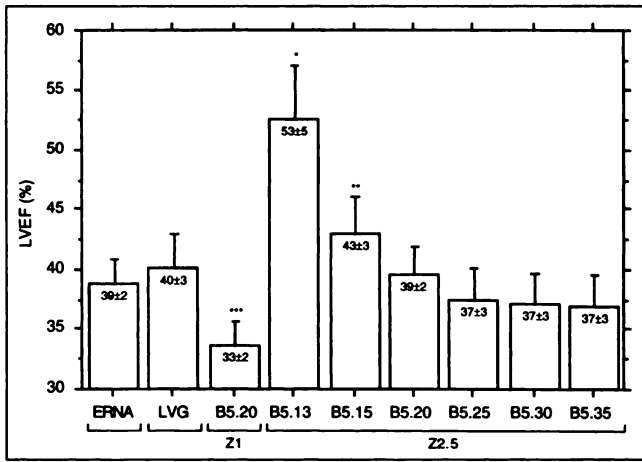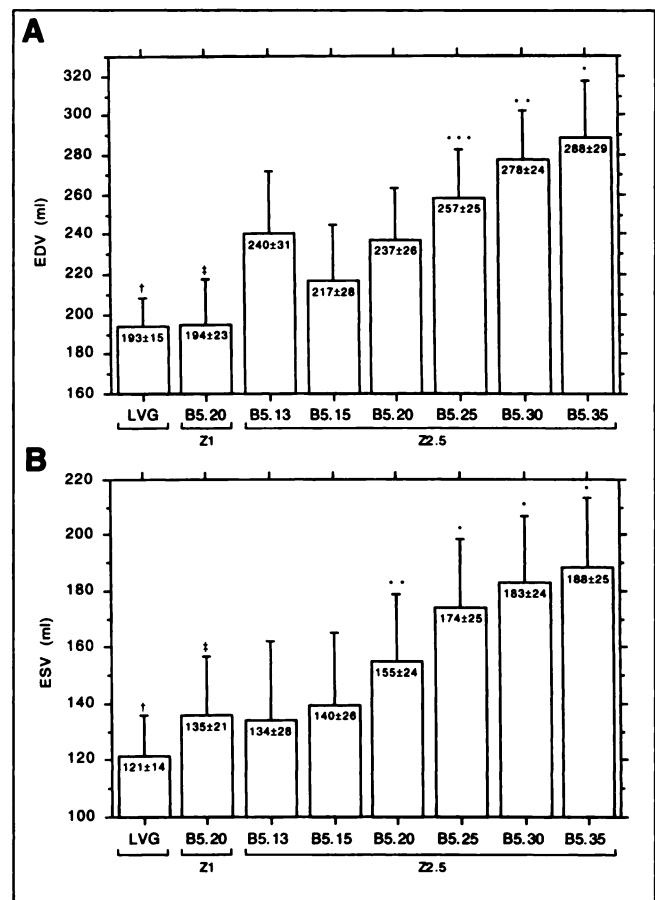
FIGURE 1. Comparison of LVEF measured by ERNA, LVG and Tl-gated SPECT. Data are mean ± SEM. *Significantly higher than all other LVEFs. **Significantly higher than B5.25, B5.30 and B5.35 LVEF. ***Significantly lower than B5.20Z2.5 LVEF.

Hanning and Butterworth filters were used in most cases. For Butterworth filters, orders ranged from 2.5 to 14, and Nyquist cutoff frequencies ranged from 0.15 to 0.33. For Hanning filters, cutoff frequencies ranged from 0.13 to 0.75 (4–6,8,9,11–13,28–36). In this study, the cutoff frequency variation of the reconstruction filter greatly influenced LVEF, EDV and ESV measurements (Figs. 1 and 2). The cutoff frequency defines the point at which the filter produces significant high-frequency suppression. Because edge has a high frequency, decreasing the cutoff frequency alters edge detection. This explains the increase in EDV and ESV when cutoff frequency increases (Fig. 2). An example is given in Figure 3. These modifications of myocardial volumes have a significant effect on LVEF measurement (Fig. 1).

With our method, Tl-gated SPECT overestimated EDV and ESV measurements compared with LVG regardless of the filter used. These results differ from those of Mochizuki et al. (6), who reported volume underestimation with gated SPECT compared with LVG. Four principal reasons may explain this difference. First, the authors used ^{99m}Tc-sestamibi or ^{99m}Tc-tetrofosmin with an injected dose of 20–30 mCi. Second, they used a low cutoff frequency for reconstruction filters (B8.15). Third, volume assessment was performed using a two-dimensional geometrical approach. Fourth, we studied a specific population with major myocardial infarction. Bland-Altman analyses showed that the overestimation of Tl-gated SPECT volumes was correlated to volume size (Table 2). To explain this result, differences between LVG and Tl-gated SPECT volumes were correlated with the infarct size (Table 3). This analysis showed that the overestimation of EDV and ESV with Tl-gated SPECT was strongly related to the infarct size for all filters (except for ESV B5.20Z1 and ESV B5.15; Table 3). (An example of regression analysis is given for B5.20Z2.5 EDV and ESV volumes in Appendix Fig. 2).

Moreover, a good contrast between myocardium and left

ventricular cavity is required for accurate edge detection with gated SPECT. To fully evaluate our results, we tested the influence of cutoff frequency on contrast. Contrast between myocardium and ventricular cavity was calculated for B5.13, B5.20 and B5.35 filters, at the site of necrosis ([necrosis − cavity]/[necrosis + cavity]) and in the normal uptake ([normal − cavity]/(normal + cavity]), in diastole and in systole (Fig. 4). Counts were measured in a 4 × 4 pixel ROI. Mean contrast did not differ between diastole and systole (0.55 ± 0.47 versus 0.50 ± 0.47; P = NS). However, with B5.13 filter, contrast greatly decreased in the necrotic region compared with the ventricular cavity. Because software defined the maxima of the first derivatives of the squared activity profiles, endocardial edge may be defined incorrectly when myocardium/cavity contrast is decreased. Therefore, reducing filter cutoff frequency decreases contrast and also alters edge detection quality, particularly in the

FIGURE 2. (A) Comparison of EDV measured by LVG and Tl-gated SPECT. Data are mean ± SEM. †Significantly lower than B5.20, B5.25, B5.30 and 5.35 EDV. ‡Significantly lower than B5.20Z2.5 EDV. *Significantly higher than B5.25, B5.20, B5.15 and B5.13 EDV. **Significantly higher than B5.20, B5.15 and B5.13 EDV. ***Significantly higher than B5.15 EDV. (B) Comparison of ESV measured by LVG and Tl-gated SPECT. Data are mean ± SEM. †Significantly lower than B5.15, B5.20, B5.25, B5.30 and 5.35 ESV. ‡Significantly lower than B5.20Z2.5 ESV. *Significantly higher than B5.20, B5.15 and B5.13 ESV. **Significantly higher than B5.13 ESV.
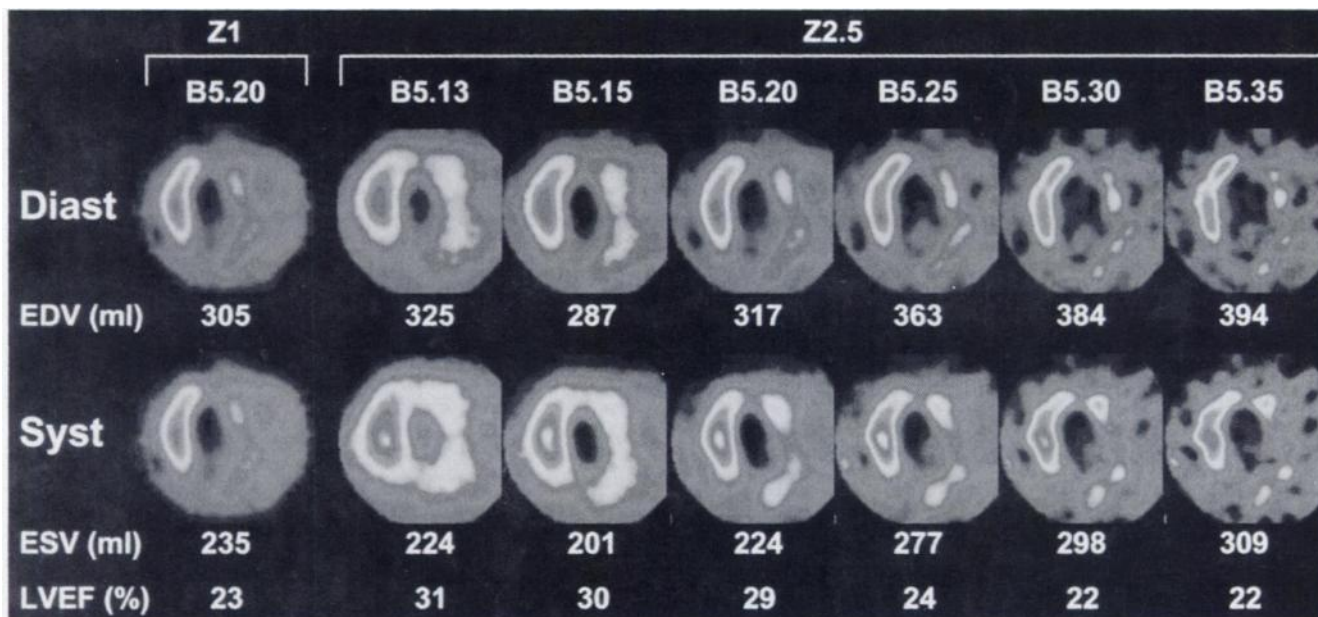
FIGURE 3. Example of effect of filtering and zooming on EDV, ESV and LVEF in patient with major myocardial infarction (diastolic [Diast] and systolic [Syst] images with zoom 1 are magnified).

necrotic region. It is suggested that very low cutoff frequencies should not be used even with Tl.

When using a small reconstruction zoom, the pixel size is high. The definition of endocardial edge is then less accurate. In this study, this phenomenon induces the underestimation of endocardial volumes, and an important underestimation of LVEF (Figs. 1 and 2). Because underestimation predominates on the EDV (Fig. 2), LVEF is therefore

underestimated. Thus, because manufacturers propose different reconstruction zooms for different gated SPECT software, caution is needed when comparing either patients or studies from different centers (or different software), even when the same reconstruction filter is used (37). Such a phenomenon probably occurs when two different acquisition zooms are used. However, this last point was not evaluated in this study.

TABLE 3
Results of Linear Regression Analysis Between LVG and Thallium-Gated SPECT Volume Differences and Infarct Size (%)

Infarct size versus	Z1	Z2.5					
	EDV–B5.20	EDV–B5.13	EDV–B5.15	EDV–B5.20	EDV–B5.25	EDV–B5.30	EDV–B5.35
a ± SE	−0.17 ± 0.04	−0.09 ± 0.31	−0.12 ± 0.04	−0.14 ± 0.04	−0.14 ± 0.04	−0.16 ± 0.04	−0.11 ± 0.03
b ± SE	36 ± 2	32 ± 3	34 ± 3	31 ± 3	27 ± 4	22 ± 4	26 ± 4
r	−0.63	−0.55	−0.52	−0.61	−0.58	−0.64	−0.57
F	15.69	10.14	8.51	13.69	12.07	16.44	11.09
P	0.0006	0.0041	0.0078	0.0011	0.0021	0.0005	0.0029
Infarct size versus	ESV–B5.20	ESV–B5.13	ESV–B5.15	ESV–B5.20	ESV–B5.25	ESV–B5.30	ESV–B5.35
a ± SE	−0.09 ± 0.07	−0.10 ± 0.04	−0.08 ± 0.05	−0.12 ± 0.05	−0.13 ± 0.05	−0.15 ± 0.05	−0.14 ± 0.04
b ± SE	35 ± 3	36 ± 3	35 ± 3.3	32 ± 3	30 ± 4	27 ± 4	27 ± 4
r	−0.28	−0.46	−0.33	−0.45	−0.47	−0.54	−0.56
F	2.06	6.32	2.84	5.92	6.49	9.71	10.92
P	0.16	0.0194	0.11	0.0232	0.0180	0.0048	0.0031

LVG = left contrast ventriculography.
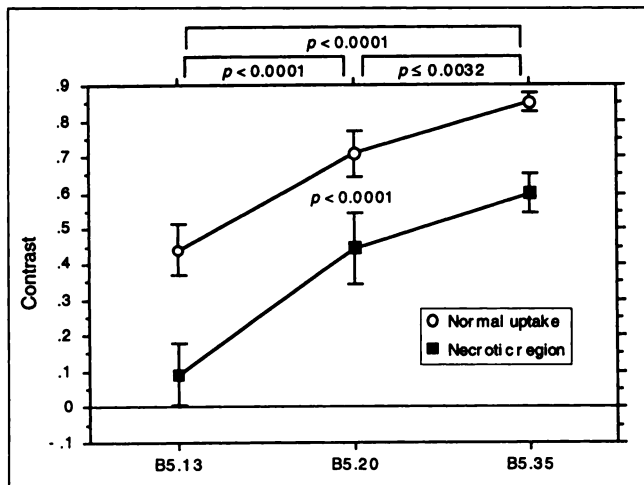EDV = end diastolic volume.
ESV = end systolic volume.
F = F value.
a ± SE = slope of linear regression ± SE.
b ± SE = intercept of linear regression ± SE.

FIGURE 4. Contrast in normal uptake regions and in necrosis with B5.13, B5.20 and B5.35 filters. Contrast was not significantly different between diastole and systole. Data are mean ± SEM.

CONCLUSION

Accurate LVEF measurements may be obtained with Tl-gated SPECT in patients with large myocardial infarction. However, filtering and zooming greatly influence EDV, ESV and LVEF measurements. Moreover, Tl-gated SPECT overestimates left ventricular volumes in patients with myocardial infarction, particularly when the infarct size is large.

APPENDIX

Appendix figures and tables mentioned in this article are on the Society of Nuclear Medicine web site at http://www.snm.org/about/jnm_abs.html. These items can be found at the end of this article's on-line abstract by clicking on the title of the article in the Table of Contents.

ACKNOWLEDGMENTS

REFERENCES

1. Lee K, Pryor D, Pieper K, et al. Prognostic value of radionuclide angiography in medically treated patients with coronary artery disease. A comparison of clinical and catheterization variables. *Circulation.* 1990;82:1705–1717.
2. Jones RH. Radionuclide angiocardiography in patients with coronary artery disease. In: Zaret BL, Beller GA, eds. *Nuclear Cardiology: State of the Art and Future Directions.* St. Louis, MO: Mosby; 1993:111–122.
3. Bonow RO. Gated equilibrium blood pool imaging: current role for diagnosis and prognosis in coronary artery disease. In: Zaret BL, Beller GA, eds. *Nuclear Cardiology: State of the Art and Future Directions.* St. Louis, MO: Mosby; 1993:123–136.
4. Germano G, Kiat H, Kavanagh PB, et al. Automatic quantification of ejection fraction from gated myocardial perfusion SPECT. *J Nucl Med.* 1995;36:2138–2147.
5. Everaert H, Franken PR, Flamen P, Goris M, Momen A, Bossuyt A. Left ventricular ejection fraction from gated SPET myocardial perfusion studies: a method based on count rate density across the myocardial wall. *Eur J Nucl Med.* 1996;23:1628–1633.

6. Mochizuki T, Murase K, Tanaka H, Kondoh T, Hamamoto K, Tauxe WN. Assessment of left ventricular volume using ECG-gated SPECT with technetium-99m-MIBI and technetium-99m-tetrofosmin. *J Nucl Med.* 1997;38:53–57.
7. Nichols K, DePuey G, Rozanski A. Automation of gated tomographic left ventricular ejection fraction. *J Nucl Cardiol.* 1996;3:475–482.
8. Williams KA, Taillon LA. Left ventricular function in patients with coronary artery disease assessed by gated tomographic myocardial perfusion images: comparison with assessment by contrast ventriculography and first-pass radionuclide angiography. *J Am Coll Cardiol.* 1996;27:173–181.
9. DePuey EG, Nichols K, Dobrinsky C. Left ventricular ejection fraction assessed from gated technetium-99m-sestamibi SPECT. *J Nucl Med.* 1993;34:1871–1876.
10. Berman D. Technetium-99m myocardial perfusion imaging agents and their relation to thallium-201. *Am J Cardiol.* 1990;66:1E–4E.
11. Maunoury C, Chen CC, Chua KB, Thompson CJ. Quantification of left ventricular function with thallium-201 and technetium-99m-sestamibi myocardial gated SPECT. *J Nucl Med.* 1997;38:958–961.
12. Germano G, Erel J, Kiat H, Kavanagh PB, Berman DS. Quantitative LVEF and qualitative regional function from gated thallium-201 perfusion SPECT. *J Nucl Med.* 1997;38:749–754.
13. Yang KTA, Chen HD. A semi-automated method for edge detection in the evaluation of left ventricular function using ECG-gated single-photon emission tomography. *Eur J Nucl Med.* 1994;21:1206–1211.
14. Rosenthal MS, Cullom J, Hawkins W, Moore SC, Tsui BMW, Yester M. Quantitative SPECT imaging: a review and recommendations by the focus committee of the Society of Nuclear Medicine Computer and Instrumentation Council. *J Nucl Med.* 1995;36:1489–1513.
15. Goris ML, Thompson C, Malone LJ, Franken PR. Modelling the integration of myocardial regional perfusion and function. *Nucl Med Commun.* 1994;15:9–20.
16. Faraggi M, Steg PG, Francois D, et al. Residual area at risk after anterior myocardial infarction: are ST segment changes during coronary angioplasty a reliable indicator? A comparison with technetium 99m-labeled sestamibi single-photon emission computed tomography. *J Nucl Cardiol.* 1997;4:11–17.
17. Véra P, Gardin I, Bok B. Comparative study of three automatic programs of left ventricular ejection fraction evaluation. *Nucl Med Commun.* 1995;16:667–674.
18. Sandler H, Dodge HT. The use of single plane angiocardiograms for the calculation of left ventricular volume in man. *Am Heart J.* 1968;75:325–334.
19. Bland JM, Altman DG. Stastistical methods for assessing agreement between two methods of clinical measurement. *Lancet.* 1986;i:307–310.
20. Boucher CA, Zir LM, Beller GA, et al. Increased lung uptake of thallium-201 during exercise myocardial imaging: clinical, hemodynamic and angiographic implications in patients with coronary artery disease. *J Am Coll Cardiol.* 1980;46:189–196.
21. Bingham JH, McKusick KA, Strauss HW, et al. Influence of coronary artery disease on pulmonary uptake of thallium-201. *Am J Cardiol.* 1980;46:821–826.
22. Levy R, Rosanski A, Berman DS, et al. Analysis of the degree of pulmonary thallium washout after exercise in patients with coronary artery disease. *J Am Coll Cardiol.* 1983; 2:719–728.
23. Gill JB, Ruddy TD, Newell JB, et al. Prognostic importance of thallium uptake by the lungs during exercise in coronary artery disease. *N Engl J Med.* 1987;317:1486–1489.
24. Villanueva FS, Kaul S, Smith WH, et al. Prevalence and correlates of increased lung/heart ratio of thallium 201 during dipyridamole stress imaging for suspected coronary artery disease. *Am J Cardiol.* 1990;66:1324–1328.
25. Beller GA. Myocardial thallium-201 imaging for detection of myocardial viability. In: Zaret BL, Beller GA, eds. *Nuclear Cardiology: State of the Art and Future Directions.* St. Louis, MO: Mosby; 1993:227–235.
26. Dilsizian V, Arrighi JA. Myocardial viability in chronic coronary artery disease: perfusion, metabolism, and contractile reserve. In: Gerson MC, ed. *Cardiac Nuclear Medicine.* New York, NY: McGraw-Hill; 1997:143–191.
27. Case JA, Cullom SJ, Bateman TM, O'Keefe JH, Williams ME. Count density and filter requirements for accurate LVEF measurements from gated Tl-201 SPECT: a gated MCAT study [abstract]. *J Nucl Med.* 1997;5:27P.
28. Faber TL, Stokely EM, Templeton GH, Akers MS, Parkey RW, Corbett JR. Quantification of three-dimentional left ventricular segmental wall motion and volumes from gated tomographic radionuclide ventriculograms. *J Nucl Med.* 1989;30:638–649.
29. Kouris K, Abdel-Dayem HM, Taha B, Ballani N, Hassan IM, Constantinides C. Left ventricular ejection fraction and volumes calculated from dual gated SPECT myocardial imaging with 99mTc-MIBI. *Nucl Med Commun.* 1992;13:648–655.
30. Chua T, Kiat H, Germano G, et al. Gated technetium-99m sestamibi for simultaneous assessment of stress myocardial perfusion, postexercice regional ventricular function and myocardial viability. Correlation with echocardiography and rest thallium-201 scintigraphy. *J Am Coll Cardiol.* 1994;23:1107–1114.

31. Germano G, Kavanagh PB, Su HT, et al. Automatic reorientation of three-dimensional transaxial myocardial perfusion SPECT images. *J Nucl Med.* 1995;36:1107–1114.

32. Anagnostopoulos C, Gunning MG, Pennell DJ, Laney R, Proukakis H, Underwood SR. Regional myocardial motion and thickening assessed at rest by ECG-gated ^{99m}Tc-MIBI emission tomography and by magnetic resonance imaging. *Eur J Nucl Med.* 1996;23:909–916.

33. Gonzalez P, Massardo T, Munoz A, et al. Is the addition of ECG gating to technetium-99m sestamibi SPET of value in the assessment of myocardial viability. An evaluation based on two-dimensional echocardiography following revascularization. *Eur J Nucl Med.* 1996;23:1315–1322.

34. Williams KA, Roberto ML, Reba RC, Taillon LA. Comparison of technetium-99m sestamibi-gated tomographic perfusion imaging with echocardiography and electrocardiography for determination of left ventricular mass. *Am J Cardiol.* 1996;77:750–755.

35. Snapper HJ, Shea NL, Konstam MA, Oates E, Udelson JE. Combined analysis of resting regional wall thickening and stress perfusion with electrocardiographic-gated technetium 99m-labeled sestamibi single photon emission computed tomography: prediction of stress defect reversibility. *J Nucl Cardiol.* 1997;4:3–10.

36. Taillefer R, DePuey EG, Udelson JE, Beller GA, Latour Y, Reeves F. Comparative diagnostic accuracy of Tl-201 and Tc-99m sestamibi SPECT imaging (perfusion and ECG-gated SPECT) in detecting coronary artery disease in women. *J Am Coll Cardiol.* 1997;29:69–77.

37. Wartski M, Gremillet E. Left ventricular ejection fraction (LVEF) assessment by myocardial gated SPECT: comparison of two methods [abstract]. *J Nucl Med.* 1997;5:27P.

38. Depuey EG, Rozanski A. Using gated technetium-99m-sestamibi SPECT to characterize fixed myocardial defect as infarct or artifact. *J Nucl Med.* 1995;36:952–955.

39. Germano G, Kavanagh PB, Berman DS. Effect of the number of projections collected on quantitative perfusion and left ventricular ejection fraction measurements from gated myocardial perfusion single-photon emission computed tomographic images. *J Nucl Cardiol.* 1996;3:395–402.